JOURNAL OF CATALYSIS 60, 460–471 (1979)

Combined Differential and Integral Kinetic Modeling in an Infrared Cell-Recycle Reactor

R. LEAUTE AND I. G. DALLA LANA[1]

Department of Chemical Engineering, University of Alberta, Edmonton, Alberta, T6G 2G6 Canada

Received January 29, 1979; revised June 5, 1979

The dehydration of 2-propanol over γ-alumina was studied at 246°C by combined *in situ* ir measurements of adsorbed species and steady-state reaction kinetics. The resulting kinetic model accounted for catalyst deactivation, product inhibition, and autoinhibition by 2-propanol. The model also predicted the integral kinetic behavior during transient (batch) operation of the reactor.

INTRODUCTION

In an earlier paper (*1*), the design of an improved infrared cell-recycle reactor and applicability to studies of mechanism and kinetics of solid-catalyzed gas-phase reactions were described. The technique is generally applicable providing: (1) the solid catalyst prepared in the form of thin wafers is sufficiently transparent to infrared (ir) radiation so that good resolution of the transmitted signal is possible; and, (2) the characteristic vibrational frequencies of adsorbed species such as reactants, products, and intermediates absorb without overlapping in the ir spectrum. The chemical reaction,

$$CH_3CH(OH)CH_3 \rightarrow CH_3C(H)=CH_2 + H_2O,$$

used in this study meets both requirements when γ-alumina is used as the solid catalyst. The reaction is irreversible under the conditions studied.

In any mechanistic interpretation of ir spectral data, it must be possible to discriminate between spectral bands originating from absorption of ir radiation in alumina itself and those of the background gas phase before observed absorption bands may be assigned to adsorbed species. Alumina surfaces are generally believed to expose Al cations, oxygen anions, and hydroxyl groups. Although Knozinger (*2*) offers a versatile model of the alumina surface, our discussion herein will be in terms of a much simpler view of the surface, one used by many workers.

In the dehydration of alcohols, olefins and ethers are both observed as products. The mechanisms involved differ in that alkoxide surface species are believed to occur when ethers are formed but not when olefins are the products (*3*, *4*). In this study, the presence of an ether product was never detected; hence, in agreement with Knozinger, we may rule out alkoxide species.

Studies involving the blocking of Lewis-acid sites on alumina by using Lewis bases (*5–7*) tend to rule out the participation of alkoxide species and/or Lewis-acid sites in the dehydration-to-olefin process. When

[1] To whom correspondence should be sent.

0021-9517/79/150460-12$02.00/0

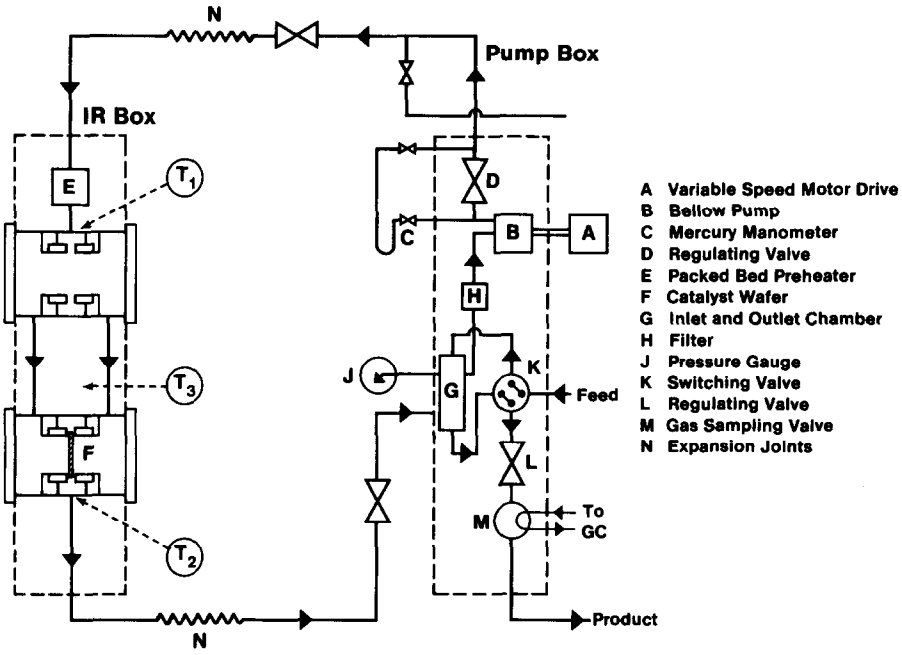

FIG. 1. Outline of ir cell-recycle reactor apparatus.

the surface basic sites were specifically blocked, the dehydration reaction (catalyst activity) was strongly inhibited (*8*). On the basis of the above points, it appears plausible to postulate that the monomolecular reaction in which an olefin is formed requires an intermediate adsorbed species in which an alcohol molecule may be bonded to both an OH group and an oxygen anion on the surface of alumina. Some lesser arguments for the involvement of a Lewis-acid site in place of the (basic) oxide site in the mechanism have been offered (*9*). More detailed studies are necessary to resolve this question of involvement of particular sites.

Corresponding detailed work on the kinetics of dehydration is either limited or absent from the literature. From kinetics and the resulting low activation energies reported in many previous publications, the question of whether the kinetics are influenced by diffusional limitations must be raised. A zero-order dependency of rate upon partial pressure of isopropanol has been reported (*10, 11*). The deuteration of the alcohol hydroxyl group did not give rise to an isotope effect whereas substitution of the β-hydrogen by deuterium produced an appreciable effect (*12*). Bremer (*13*) noted that the initial rate of dehydration of isopropanol decreased with increasing partial pressure of the alcohol. In terms of a simplified homogeneous surface, this rate-retarding effect may be explained in terms of a dual-site mechanism via

$$r_0 = kK_AP_A/(1 + K_AP_A)^2.$$

It is evident that the kinetics of this reaction has not really been developed conclusively nor studied extensively at other than relatively low conversions. The use of a recycle reactor, the basis of this work, enables a much wider range of conversions to be examined.

EQUIPMENT AND TECHNIQUE

Reactor

General details of the ir cell-recycle reactor have been provided (*1*). Figure 1 shows the reactor, pump, ovens, and the related piping. The two ovens were controlled at the reaction temperature (up to

400°C) and at 220°C, respectively. The heating of the reactor oven was regulated by measurement of the temperature of the combined gas flows impinging on both sides of the catalyst wafer, T_2. The oven temperature was maintained within 0.5°C of the wafer temperature, T_2, by circulating heated air. During the kinetics measurements under steady-state operation, the cell reactor was withdrawn from the sample compartment because the changing absorption of ir radiation by the wafer during a spectral scan could change the wafer temperature by a few degrees. Changing one valve setting converted the operating mode instantaneously from open (flow) to closed (batch) recycle.

In the closed mode, the transient operation could be followed by monitoring a specific absorption band (not overlapping with other bands) continuously; thus the wafer temperature was not altered by ir absorption. On the other hand, the recycling gas temperature was affected up to 2°C by the change in thermal properties of the gases with changing composition.

The recycle stream was pumped using a Metal Bellows high-temperature stainless-steel pump (Model MB-118HT). Recirculation rates were tested to ensure that the volumetric flows were large enough to eliminate external mass transfer limitations. Earlier experience from varying the thickness of the alumina wafer indicated that the ~0.1 × 25-mm wafer should not encounter pore diffusion limitations. Measurements under these conditions should provide intrinsic rates of reaction.

The liquid 2-propanol feed was regulated using a Sage Model 355 syringe pump. Although the syringe pump introduced minute flow pulses discernible over short-term periods, the overall steady-state performance was reproducible over the duration of a run, generally from 0.5 to 1 h. The feed flow rate was calculated using gc analysis of the N_2–propanol feed mixture and the carefully metered N_2 flow rate. This combined feed was preheated to the pump box temperature before entering the reaction loop. A small packed bed of glass beads located before the cell inlet provided the preheat temperature control at T_1.

Analytical Method

The accuracy of ir absorption quantitative analysis of the gas-phase streams was less than that obtainable by gc techniques. Both feed (N_2 and 2-propanol) and product (propylene, water, N_2, and 2-propanol) stream compositions were determined by gc separation.

The conversion of 2-propanol to propylene was calculated using the alcohol–N_2 ratios in both feed and product streams. The water and propylene product stream contents usually checked within 3% of each other. The feed reagents, isopropanol (Fisher C. P. grade), N_2 gas (99.99% specs.), and distilled water, were used as obtained. Alumina (ALON, Cabot Corp.) was compressed into very thin wafers by compaction at 10 ton in.$^{-2}$ in a 1-in. diameter die.

Infrared Technique

Complete ir spectral scans or continuous monitoring at specific ir frequencies were obtained using a Perkin–Elmer Model 621 infrared spectrophotometer. The ir cell-recycle reactor was designed to fit into the sample compartment to enable double-beam transmission through the NaCl windows of the two cylinders in the loop. In this way, direct internal compensation for background gas-phase spectra was achieved. The recorded spectral scans were representative of the baseline of the solid alumina plus absorption bands attributable to adsorbed species. Emission spectra, if any, were filtered electronically by chopping the incident beam before transmission through the wafer.

EXPERIMENTS: MECHANISM

Complete spectral scans were recorded during steady-state tests during which all

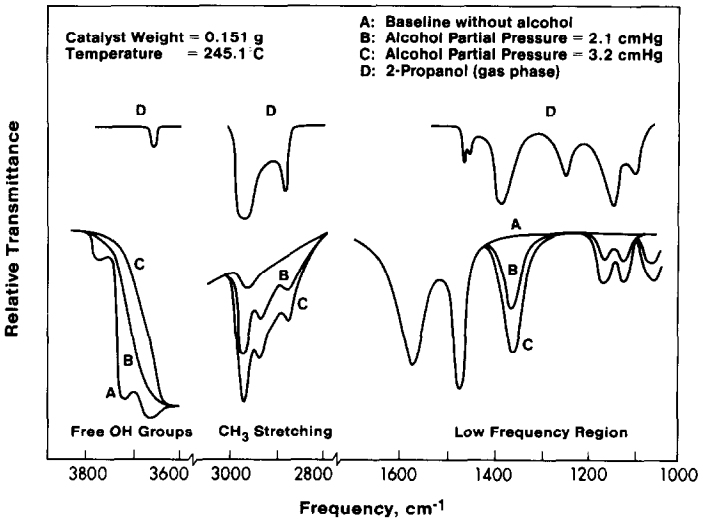

FIG. 2. Infrared spectral evidence for adsorbed species in dehydration of 2-propanol on γ-alumina (ALON).

experimental parameters (T, P, flows, pump speed) were held constant. Absorption bands thus recorded were compared to gas-phase spectra for each component and to spectra in the literature taken under similar conditions. Figure 2 summarizes the noteworthy regions of the ir spectrum in which spectral bands for the adsorbed species were interpreted. Discussion of regions of the spectrum not of consequence in this work has been omitted.

The criterion initially employed for associating band character with adsorbed species likely involved in the dehydration reaction mechanism was to observe if changes in concentration of 2-propanol in the feed also influenced intensities of particular bands. Constancy of the band intensity when the reaction rate was so changed presumed independence from the surface reaction of interest. (This criterion is not infallible, e.g., as will be seen, the 2-propanol adsorbs as a reactant and although the intensity of the 2970 cm^{-1} band changes, the reaction rate remains constant. However, both do change simultaneously at low surface coverages of 2-propanol.) Spectral bands associated with spurious adsorbed species (using the above criterion) were examined to determine if they independently influenced the reaction rate.

Returning to Fig. 2, one notes:

(1) The surface hydroxyl groups (3600–3800 cm^{-1}) associated with the alumina surface progressively disappear with increasing 2-propanol concentration. This suggests that the hydroxyl site may indeed be a surface reaction site via some form of hydrogen bonding. Intuitively, the stability of such bands at reaction temperatures (~240°C) may be questioned and thus, one also questions whether the adsorbed species truly chemisorb on the hydroxyl sites.

(2) The stretching vibrations of the methyl groups in 2-propanol (2800–3000 cm^{-1}) change in band intensity directly with changes in 2-propanol concentration.

(3) In the low-frequency region, the 1000–1200 cm^{-1} bands related to carbon chain skeletal vibrations also change.

(4) And, also in the low-frequency region, the ~1350 cm^{-1} band related to C–H symmetrical deformation vibrations in the methyl groups increases with increasing 2-propanol concentration. A com-

parison between the different C–H stretching bands of liquid 2-propanol (2970 cm^{-1} = CH_3 antisymmetric (I); 2930 cm^{-1} = C–H stretching (II); 2870 cm^{-1} = CH_3 symmetric stretching (III)) with the corresponding bands of the adsorbed alcohol may be relevant. In the liquid, bands II and III exhibit similar intensities. For the adsorbed state, band II is nearly double the intensity of band III, suggesting that the symmetric stretching mode had been somewhat hindered. This may be explained by assuming that the alcohol molecule adsorbs not only by bonding of the OH group but also via a bond with a β-hydrogen atom. In effect, this eliminates half of the symmetric contributions from the two methyl groups, which is also approximately the magnitude of the reduction in the 2870 cm^{-1} band.

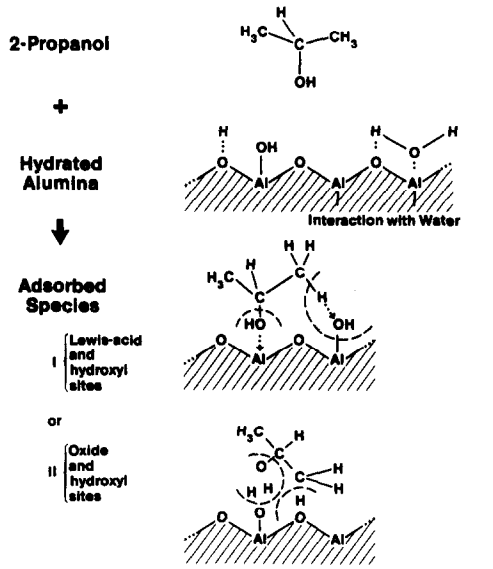

FIG. 3. Nature of surface reaction. Mechanistic view of gas-phase chemical steps.

(5) The two bands in the region 1400–1600 cm^{-1} do not change with 2-propanol concentration changes and it may be surmised that they are not involved in the reaction mechanism. These bands have previously been assigned (*14*) to an irreversibly adsorbed carboxylate species.

On the basis of these observations and, to a lesser extent, implications from the kinetics, Fig. 3 depicts a reaction mechanism in accord with the above.

EXPERIMENTS: KINETICS

Measurement of Differential Rates

All rate measurements were obtained at a wafer temperature of 246.5°C using an 86-mg wafer of alumina. Plotting the absorbance of the 2970 cm^{-1} band of 2-propanol (related to its surface concentration) against the partial pressure of the alcohol obtained from various steady-state runs at constant total feed rate and reaction pressure yielded Langmuir-type adsorption isotherms. Interference from the CH_3-stretching vibrations of the carboxylate species, also at 2970 cm^{-1}, was not observed. These "isotherms" recorded at reaction conditions increased in slope near the origin when the temperature was lowered. In fact, at 210°C, the saturation level of 2-propanol surface coverage was reached before any practical level of partial pressure of 2-propanol was attained within the cell. Above 280°C, the absorbance was too small to provide reliable information. This range of temperatures confined the region in which steady-state spectra could be obtained along with differential reaction rates. Reaction rates may be obtained outside of this 210–280°C temperature range but without supporting ir evidence.

Rates would be calculated directly using the material balance equation for an ideal stirred-tank reactor. A number of preliminary aspects were examined prior to being able to measure intrinsic reaction rates.

Changes in Catalytic Activity

Constancy of the catalytic activity of alumina was required during the kinetics runs and a number of influences were encountered and examined.

1. Carboxylate adsorbed species. Figure 4

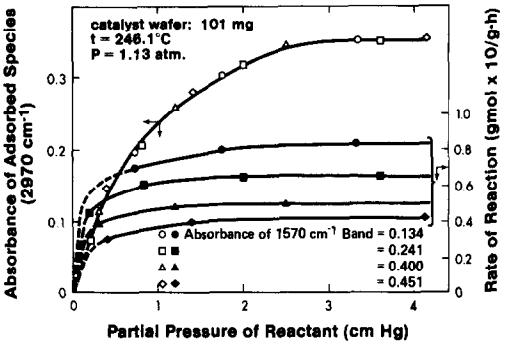

FIG. 4. Influence of carboxylate surface species upon observed rates of reaction.

shows that the reaction rates at similar conditions decline visibly when the absorbance of the 1570 cm^{-1} band of carboxylate species increased. The adsorption isotherm for 2-propanol, obtained by measuring the absorbance of the 2970 cm^{-1} band of 2-propanol, shows that all such absorbances are correlated by a single isotherm irrespective of the carboxylate species' surface concentration (1570 cm^{-1}). In all cases, the rate became limited upon attaining a saturation level of surface 2-propanol. This saturation level declined with increasing carboxylate concentration.

The carboxylate species appeared upon heating the catalyst in the presence of 2-propanol and could be removed by exposure to O_2 above 350°C. A stable carboxylate surface population (absorbance) could be attained for the runs by pretreating at a temperature above 246°C with a specified partial pressure of 2-propanol and then by making all runs at the lower temperature, 246.5°C.

Since the carboxylate level did not influence the surface coverage of alcohol but affected the reaction rate adversely, this was interpreted to mean that the carboxylate and alcohol adsorbed on different sites. To account for the detrimental influence of the carboxylate species, they are presumed to occupy sites which are adjacent to the 2-propanol adsorption sites, and which are essential for the reaction to occur. It has been suggested by a reviewer that these additional adjacent sites might be basic OH sites which are essential for β-hydrogen abstraction from 2-propanol. Elimination of basic OH sites by being consumed in the formation of the surface carboxylate species would account for the poisoning role of the surface carboxylate species.

2. Influence of products. Although the dehydration reaction appeared to be irreversible, the influence of the presence of reaction products was also investigated. Addition of propylene to the feed produced no observable effect upon the reaction rate. Its presence on the surface of alumina at reaction conditions could not be detected by ir methods.

The addition of water to the feed generated the results shown in Fig. 5. The adverse effect of water and the unaffected adsorption isotherm of 2-propanol also suggests that adsorption of water occurs on a site other than the type for alcohol adsorption.

Since both water and carboxylate retard reaction rates well before the adsorption sites for 2-propanol become saturated, it may be assumed that the total population of alcohol adsorption sites, L_1, greatly exceeds the total population of the adjacent required different sites, L_2. Removal of a few l_2-type sites by adsorption of water or formation of carboxylate suppresses the

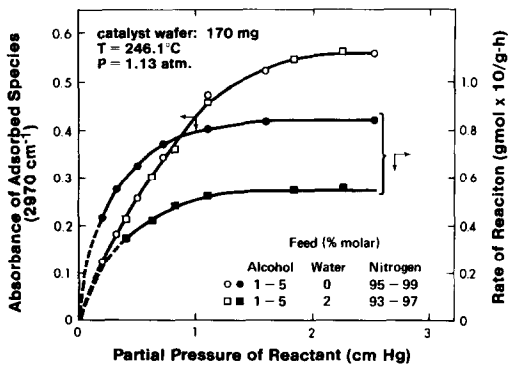

FIG. 5. Influence of water (product) upon observed rates of reaction.

reaction rate disproportionately (evidence that the surface is heterogeneous).

The experimental rates of reaction (27 data points) shown in Fig. 6 indicate not only the retarding influence of water but also, that the reaction rate exhibits a maximum and eventually levels off (~zero order in 2-propanol). The nature of the adsorption of alcohol somehow must account for the maxima observed. The explanation may be, in terms of the two types of sites, l_1 and l_2, that if adsorption of one or more alcohol molecules on one or more l_1 sites surrounding a single l_2 site could increasingly sterically hinder adsorption of another alcohol molecule upon an l_1 site adjacent to the l_2 site in question, access of any adsorbed alcohol molecule to the adjacent l_2 site becomes increasingly difficult. Accordingly, the reaction rate would be expected to decrease. When saturation of the surface by alcohol is approached, this situation could become regulatory. (In other words, if a fraction of the l_2 sites are sterically hindered, this fraction may be proportional to the degree of saturation of l_1 sites by isopropanol.)

Reaction Mechanism and Rate Equation

The mechanism advanced in Fig. 3 for the irreversible dehydration of isopropanol may be described by the following elementary steps,

$$A + l_1 \rightleftarrows A \cdot l_1, \tag{1}$$

$$A \cdot l_1 + l_2 \rightarrow P + W \cdot l_2 + l_1, \tag{2}$$

$$W \cdot l_2 \rightleftarrows W + l_2. \tag{3}$$

Assuming the surface reaction (2) to be irreversible and rate controlling, the mechanism implies a rate equation of the form

$$r = \frac{k_2 K_1 L_1 L_2 P_A}{(1 + K_1 P_A)(1 + P_w/K_3)}. \tag{4}$$

Equation (4) must be modified if the various rate-retarding influences are to be accommodated.

The population of the carboxylate-adsorbed species was held constant (maintain constant intensity of the 1570 cm^{-1} band during the set of experiments). Physically, this is equivalent to reducing the total population of l_2 sites via a fraction, α_c, such that

$$L'_2 = \alpha_c \cdot L_2, \tag{5}$$

where α_c is a constant fraction at a given temperature.

The denominator term in Eq. (4) will account for the rate-retarding influence of water. Apparently water adsorbs strongly whereas the other product, propylene, adsorbs negligibly.

The retarding influence of alcohol is less evident. From mass law considerations, the irreversible surface reaction step (2) may be described by the rate equation

$$r_2 = k_2[A \cdot l_1][l_2]. \tag{6}$$

To explain the maxima shown in Fig. 6, note that the surface concentration of the adsorbed alcohol, $[A \cdot l_1]$, is also plotted against partial pressure of 2-propanol, rising continuously toward saturation. To explain this maximum in the rate and its leveling off, $[l_2]$ must be decreasing. This decrease in $[l_2]$ eventually more than compensates for the increase in $[A \cdot l_1]$ causing r_2 to exhibit a maximum. Using the steric hindrance explanation offered earlier, the alcohol is seen to be autoinhibiting. Pursuing this line of thought, and in the absence of other explanations, assume that a constant fraction of $[A \cdot l_1]$ adsorbed entities, ϕ, is responsible for the steric hindrance of the adjacent l_2 sites. This is reasonable if the populations, L_1 and L_2, do not change. Then, the concentration of the sterically hindered sites, $[l'_2]$, is given by

$$[l'_2] = \phi \cdot [A \cdot l_1], \tag{7}$$

where, $0 \leq \phi \leq 1$. The surface balance equation for l_2 sites becomes

$$L_2 = [l_2] + [W \cdot l_2] + [l'_2].$$

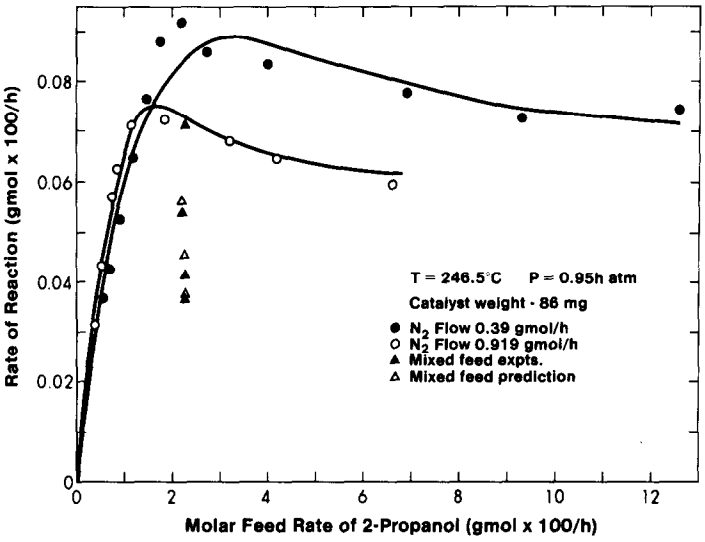

FIG. 6. Comparison between experimental and simulated differential rates of reaction.

Substituting for the terms in the RHS, we obtain

$$[l_2] = L_2 \frac{[1 + K_1P_A(1 - \phi(L_1/L_2))]}{[1 + K_1P_A][1 + P_W/K_3]}.$$

Note that the term, $(1 - \phi(L_1/L_2))$, does not represent a fraction between 0 and 1 because $(L_1/L_2) > 1$. Upon substitution, Eq. (4) changes to the form

$$r = \frac{k_2K_1L_1L_2P_A[1+K_1(1-\phi(L_1/L_2))P_A]}{[1+K_1P_A]^2[1+P_W/K_3]}, \tag{8}$$

and upon lumping constants,

$$a = k_2K_1L_1L_2, \quad c = 1/K_3,$$
$$b = K_1, \quad d = K_1(1 - \phi(L_1/L_2)),$$

$$r = \frac{aP_A(1 + dP_A)}{(1 + bP_A)^2(1 + cP_W)}. \tag{9}$$

INTERPRETATION OF KINETICS

Kinetic Model

In addition to the model developed, (8), a number of other empirical and semi-empirical rate equations were considered. The majority could be quickly eliminated because of their contradictions to the chemical evidence described herein. A few remaining empirical models were discarded after attempting to estimate their parameters. The Marquardt algorithm was used in searching for the parameter values which best satisfied a nonlinear least-squares criterion.

Referring to Fig. 6, the experimental data for the present comprise three sets of points, 13, 10, and 4, or a total of 27 points. Using the sets, cumulatively, 13, 23, and 27 points, the parameter values estimated are shown in Table 1.

The quality of fit using the final set of parameters is indicated by the solid line in Fig. 6, which was obtained by calculating rates using Eq. (9). The addition of the autoinhibition term results in an equation which fits rather well. With minor refinements and additional data obtained at statistically significant regions, a very good model should result. Ultimately, this model will provide the basis for attempting to correlate the kinetics over a range of temperatures.

Since the above exercise merely reflects the ability of the model "to regenerate

TABLE 1

Parameter Estimation for Equation (9)

$$r = \frac{aP_a(1 + dP_a)}{(1 + bP_a)^2(1 + cP_w)}$$

Data set	a	b	c	d
1. Initial 10 points	2.24 ± 0.935	198.6 ± 289.9	23.98 ± 21.87	71.90 ± 159.58
2. 23 points	2.737 ± 0.333	78.34 ± 15.73	23.88 ± 12.24	13.61 ± 6.56
3. 27 points (4 mixed feed)	2.826 ± 0.289	77.07 ± 14.15	29.56 ± 8.59	13.06 ± 5.85

$\sigma^2 = 1.92 \times 10^{-7}$

itself," an additional experiment involving different experimental conditions was performed using transient rather than steady-state kinetics.

Measurement of Batch Conversions

1. Procedures. The recycle loop was designed to be enabled to switch from open to closed (or vice versa) operating modes instantaneously. Starting from a steady-state situation, ir data were recorded continuously at a fixed chart speed. The 1140 cm^{-1} band of gas-phase isopropanol was calibrated to obtain its extinction coefficient within 5% accuracy. To monitor this band, the reference side of the cell reactor was positioned in the sample side of the infrared spectrophotometer. Monitoring this band using single-beam attenuation by the gas phase provided the concentration of 2-propanol.

By eliminating sampling the mass of the system remained constant during the batch operation. Because the two ovens in the loop operated at different temperatures, the constant volume loop is not at a uniform temperature. This temperature gradient within the loop complicates the determination of the circulating number of gram moles at any instant. The resolution of this problem required some additional experiments.

To provide the value of M_t, the number of moles in the batch system at time t, the procedure requires knowledge of the flow rate of N_2 entering an open loop (through which only N_2 and water are passed) and the mole fraction of water in the feed at the outset of the experiment. The reactor was operated at the same temperature and pressure anticipated in subsequent kinetics runs, but with a continuous nonreactive N_2–H_2O feed mixture. At $t = 0$, the water was switched off but N_2 flow maintained. The transient decay of $[H_2O]$ in the loop was determined by gc sampling and analysis at 70-s intervals.

At time t, the mass balance for H_2O in the reactor is

$$\dot{M}(0 - x_W) = M_t \frac{dx_W}{dt}, \qquad (10)$$

in which $\dot{M}$ is the molar flow of N_2 through the loop. Integrating between $t = 0$ and $t = t$, $x_W = x_{W1}$ and $x_W = x_{W2}$, obtain

$$M_t = \text{constant} = -\dot{M}(\Delta t)/\log (x_{W2}/x_{W1}). \qquad (11)$$

Applying this equation to any transient period, Δt, should give the same value, M_t. The values, M_t, so obtained were averaged and used in the analysis of the transient kinetic data.

2. Integral equation for batch reactor. Consider the following stoichiometric calculations for the dehydration reaction,

$$A \rightarrow P + W,$$

in which the desired mole fraction, x_i, is to be expressed in terms of M_0, the original

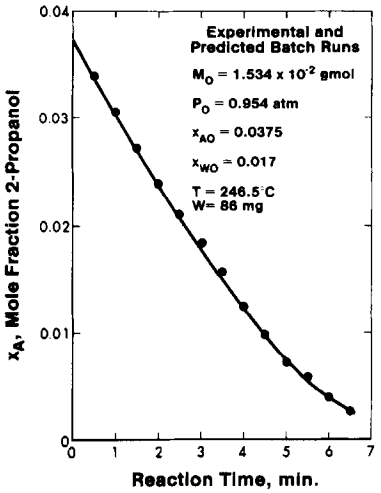

FIG. 7. Comparison between experimental and predicted behavior of batch catalytic reactor.

number of moles in the loop at the start of the batch reactor operation, and M_t, the corresponding number of moles at a time, t, later. Defining,

$$X = \text{(moles of A converted)/(moles of A initially present)} = (M_0 x_{A0} - M_t x_A)/M_0 x_{A0}). \quad (12)$$

Using, $M_t = M_0 + M_0 x_{A0} X$, rearrange (12) to obtain,

$$X = \frac{x_{A0} - x_A}{x_{A0}(1 + x_A)}. \quad (13)$$

Upon introducing this into the isothermal differential material balance equation for a batch reactor,

$$M_t \frac{dX}{dt} = W \frac{aP_A(1 + dP_A)}{(1 + bP_A)^2(1 + cP_W)}, \quad (14)$$

and after substituting to eliminate M_t and X, obtain

$$dt = \frac{M_0(1 + b'x)^2(c' + c''x)}{W(a'x)(1 + x)^2(1 + d'x)} dx, \quad (15)$$

where

W = weight of catalyst in loop,
$a' = aP_0$,
$b' = 1 + bP_0(1 + x_{A0})$,
$c' = 1 + cx_{A0} + cx_{W0}P_0$,
$c'' = 1 - c + cP_0x_{W0}$,
$d' = 1 + dP_0(1 + x_{A0})$.

Now, knowing the initial conditions for a batch run and the parameters in the rate expression (9), the five constants, $a', \ldots, d'$, may be evaluated. M_0 was obtained from the N_2–H_2O transient experiment for the same recycle loop pressure and temperature distribution.

A batch experiment has been plotted in the form, x_{A0} vs t, in Fig. 7. The experimental points show very good agreement with the predicted curve obtained by integrating Eq. (15) numerically.

CONCLUSIONS

1. The use of the infrared cell-recycle reactor has eliminated considerable empiricism from the kinetic modeling of the catalytic dehydration of 2-propanol. The interpretive rate expression developed in this work provided means of accounting for catalyst deactivation, product inhibition of the rate, and autoinhibition by a reactant. The recommended isothermal expression at 246.5° is

$$r = \frac{2.826P_A[1 + 13.06P_A]}{[1 + 77.07P_A]^2[1 + 29.56P_W]} = \text{g mol/(g cat)(sec)}.$$

2. This method of "chemical insight," perhaps onerous in use of auxiliary evidence and techniques, facilitates direct progress in kinetic modeling through elimination of competing models on the grounds of chemical incompatibility.

3. Use of a combined-mode recycle reactor enables differential or integral treatment of experimental kinetics data, whichever is more convenient, and provides a more stringent test of models than by "simple" regeneration of the parent data.

4. The dehydration of 2-propanol is much better understood from such studies, perhaps in terms of gas-phase molecules, but the role of the surface of the catalyst remains much more clouded. The combination of ir and kinetics with a third experimental technique delineating the surface character, preferably under reac-

tion conditions, should provide a very powerful approach.

5. This study needs to be extended to a range of temperatures and more extreme sets of operating conditions in both open and closed reaction modes to demonstrate definitively that rate expressions obtained in this manner have general applicability.

APPENDIX: NOMENCLATURE

A, P, W	Designates alcohol, propylene, and water molecules, respectively; also used in subscripts
$A \cdot l_1$	Adsorbed species formed by A on active site, l_1
a, b, c, d a', b', c', d', c''	Lumped constants
k_i	Rate constant for the forward reaction in the ith elementary step in the mechanism
K	Equilibrium constant for the overall reaction
K_A, K_1, K_2	Equilibrium constants for adsorption of specific chemical species on the catalyst surface
l_1, l_2	Denotes active sites of types 1 and 2, respectively
L_1, L_2, L'_2	Total populations of the particular types of site on the specified mass of catalyst
$\dot{M}$	Mass flow rate of nitrogen, g mol/time
M_0	Total g mol in batch reactor at a time, $t = 0$
M_t	Total g mol in given reactor at specified time, $t = t$
P_A, P_W	Partial pressures of components in gas phase, atm
r	Rate of reaction, g mol reacted/(g catalyst) (h)
X_A	A (mol) converted per mole of A initially present
x_A, x_{A0}, x_W	Mole fraction of particular species (subscript zero refers to start of batch reaction)
W	Catalyst (g) in recycle reactor
$W \cdot l_2$	Adsorbed species formed by W on active site, l, of a particular type
α_c	Fraction of sites which have been blocked off by the carboxylate-adsorbed species
ϕ	Ratio of concentration of hindered sites of type l_2 to concentration of adsorbed alcohol on sites of type l_1
Δt	Increment in time, during special test to evaluate M_t

ACKNOWLEDGMENTS

Financial support provided by the National Research Council of Canada, the Canada Council, and the University of Alberta is gratefully acknowledged.

REFERENCES

1. Leaute, R., and Dalla Lana, I. G., *in* "Chemical Reaction Engineering—Houston" (V. W. Weekman and D. Luss, Eds.), ACS Symposium Series, Vol. 65, p. 3. Amer. Chem. Soc., Washington, D.C., 1978.
2. Knozinger, H., *Catal. Rev. Sci. Eng.* **17**, 31 (1978).
3. Knozinger, H., Bühl, H., and Ress, E., *J. Catal.* **12**, 121 (1968).
4. Treibmann, D., and Simon, A., *Ber. Bunsenges. Phys. Chem.* **70**, 562 (1966).
5. Yakerson, V. I., and Lefer, L. I., *Dokl. Acad. Nauk Uzb. SSR* **174**, 11 (1976).
6. Misamo, M., Saito, Y., and Yaneda, Y., *in* "Proceedings. 3rd International Congress on Catalysis, Amsterdam, 1964" (W. M. H. Sachtler, G. C. A. Schiut, and P. Zwietering, Eds.), p. 408. North-Holland, Amsterdam, 1965.
7. Knozinger, H., *Angew. Chem. Int. Ed. Engl.* **7**, 791 (1968).

8. Knozinger, H., and Stolz, H., *Ber. Bunsenges. Phys. Chem.* **74**, 1056 (1970).

9. Figueras Roca, F., de Mourgues, L., and Trambouze, Y., *C. R. Acad. Sci., Ser. C* **266**, 1123 (1968).

10. Bremer, H., Steinberg, K. H., Glietsch, J., Lasky, H., Werner, U., and Wendlandt, K. D., *Z. Chem.* **10**, 5 (1971).

11. de Mourgues, L., Peron, F., Trambouze, Y., and Prettre, M., *J. Catal.* **7**, 117 (1967).

12. Knozinger, H., and Scheglila, A., *J. Catal.* **17**, 252 (1970).

13. Knozinger, H., Krietenbrink, H., Miller, H. D., and Schulz, W., *in* "Proceedings. 6th International Congress on Catalysis, London, 1976" (G. C. Bonds, P. B. Wells, and F. C. Tompkins, Eds.), p. 183. The Chemical Society, London, 1977.

14. Deo, A. V., Chuang, T. T., and Dalla Lana, I. G., *J. Phys. Chem.* **75**, 234 (1971).